Constrained Connectivity and Transition Regions

Pierre Soille[1] and Jacopo Grazzini[2]

[1] Institute for the Protection and the Security of the Citizen
Global Security and Crisis Management Unit
[2] Institute for Environment and Sustainability
Spatial Data Infrastructures Unit
European Commission, Joint Research Centre
T.P. 267, via Fermi 2749, I-21027 Ispra, Italy

Abstract. Constrained connectivity relations partition the image definition domain into maximal connected components complying to a series of input constraints such as local and global intensity variation thresholds. However, they lead to a stream of small transition regions in situations where the edge between two large homogeneous regions spans over several pixels (ramp discontinuity). In this paper, we analyse this behaviour and propose new definitions for the notions of transition pixels and regions. We then show that they provide a suitable basis for suppressing connected components originating from non ideal step edges.

1 Introduction

Owing to the natural one-to-one correspondence between the partitions of a set and the equivalence relations on it [1, p. 130] and given that connectivity relations are equivalence relations, image segmentation [2] based on logical predicates defined in terms of connectivity relations naturally leads to uniquely defined image partitions[1]. For example, the trivial connectivity relation stating that two pixels are connected if and only if they can be joined by an iso-intensity path breaks digital images into segments of uniform grey scale [4]. They are called plateaus in fuzzy digital topology [5] and flat zones in mathematical morphology [6]. In most cases, the equality of grey scale is a too strong homogeneity criterion so that it produces too many segments. Consequently, the resulting partition is *too fine*. A weaker connectivity relation consists in stating that two pixels of a grey tone image are connected if there exists a path of pixels linking them and such that the grey level difference along adjacent pixels of the path does not exceed a given threshold value. In this paper, we call this threshold value the local range parameter and denote it by α. Accordingly, we call the resulting connected components the α-connected components. This idea was introduced in image processing by Nagao, Matsuyama, and Ikeda in the late seventies [7] but was already known before in classification as the single linkage clustering method [8].

[1] Partial partitions relying on partial equivalence relations (i.e., symmetric and transitive relations that are not necessarily reflexive) are studied in [3].

M.H.F. Wilkinson and J.B.T.M. Roerdink (Eds.): ISMM 2009, LNCS 5720, pp. 59–69, 2009.

α-connected components are called quasi- or λ-flat zones [9,10] in mathematical morphology. Although α-connected components often produce adequate image partitions, they fail to do so when distinct image objects (with variations of intensity between adjacent pixels not exceeding α) are separated by one or more transitions going in steps having a magnitude less than or equal to α. Indeed, in this case, these objects appear in the same α-connected component so that the resulting partition is *too coarse*. This problem is sometimes referred to as the 'chaining effect' of the single linkage clustering method [11]. A natural solution to this problem is to limit the difference between the maximum and minimum values of each connected component by introducing a second threshold value called hereafter global range parameter and denoted by ω. This led to the notion of constrained connectivity introduced in [12]. A more general framework where constraints are defined in terms of logical predicates is put forward in [13]. Constrained connectivity solves the chaining effect of α-connectivity because appropriate global constraints prohibit α-connected components to grow too much. However, it may create a series of small undesirable regions in situations where the edge between two homogeneous regions spans over several pixels in the form of a ramp discontinuity [14]. This motivated us to analyse this behaviour and propose appropriate definitions for the notions of transition pixels and regions. They provide a basis to suppress all connected components originating from non ideal step edges[2], see also preliminary results in [15].

Section 2 briefly recalls the notion of constrained connectivity expressed in terms of logical predicates. Transitions pixels and regions are studied in Sec. 3. Before concluding, experimental results are presented in Sec. 4.

2 Logical Predicate Connectivity

We define $\boldsymbol{\alpha}$-connectivity for multichannel images following [7] (see also [16] where $\boldsymbol{\alpha} = (\alpha_1, \ldots, \alpha_m)$ is referred to as the differential threshold vector): if, for every channel j, the difference of the values between two adjacent pixels is less than or equal to α_j, then the two pixels belong to the same component. Equivalently, denoting by f_j a scalar image, two pixels p and q of a multichannel image $\mathbf{f} = (f_1, \ldots, f_m)$ are $\boldsymbol{\alpha}$-connected if there exists a path $\mathcal{P} = (p = p_1, \ldots, p_n = q)$, $n > 1$, such that $|f_j(p_i) - f_j(p_{i+1})| \leq \alpha_j$ for all $1 \leq i < n$ and for all $j \in \{1, \ldots, m\}$. By definition, a pixel is $\boldsymbol{\alpha}$-connected to itself. If necessary, a more general definition whereby the component-wise grey level difference is replaced by an arbitrary distance on vectors [10,17,18] can be considered. For instance, the Mahalanobis distance provides us with a scale-invariant distance taking into account the correlations between the different channels. Alternatively, one could define the $\boldsymbol{\alpha}$-connected component of a pixel by computing the intersection of the α_j-connected components obtained for each channel separately and then extract the connected component of this intersection that contains this pixel. In practice, because the connections between pixels may follow different paths in each channel, it may be necessary to consider the intersection of graphs rather

[2] An ideal step edge consists of a discontinuous jump from one value to another.

than just an intersection on the nodes of the connected components obtained for each channel. This will be detailed in a future paper.

To determine whether two vectors are ordered, we use the marginal ordering [19] and denote by $\preceq$ the resulting relation 'less than or equal to': $\mathbf{f}(p) \preceq \mathbf{f}(q) \Leftrightarrow \mathbf{f}_j(p) \leq \mathbf{f}_j(q)$ for all $j \in \{1, \ldots, m\}$. Nevertheless, the family of partitions into $\boldsymbol{\alpha}$-connected components, for varying $\boldsymbol{\alpha}$, is not totally ordered because of the absence of total ordering between the vectors α_i such that $\boldsymbol{\alpha}_i \preceq \boldsymbol{\alpha}$. We solve this problem by authorising only local vector range parameters having the same range α for all channels (so that it comes down to a unique scalar value α). In practice, this is not a limitation because the individual channels of the input multichannel image can be transformed beforehand.

Recall that a logical predicate P returns true when its argument satisfies the predicate, false otherwise. In general, provided that a given predicate returns true on iso-intensity connected components, we may look for the largest α_i-connected component satisfying this predicate such that every α_j-connected component where $\alpha_j \leq \alpha_i$ also satisfies it. This leads to the following general definition when considering a series of n predicates returning true when applied to iso-intensity connected components:

$$(P_1, \ldots, P_n)\text{-CC}(p) = \tag{1}$$
$$\bigvee \Big\{ \alpha_i\text{-CC}(p) \;\Big|\; P_k\Big(\alpha_i\text{-CC}(p)\Big) = \text{true for all } k \in \{1, \ldots, n\} \text{ and}$$
$$P_k\Big(\alpha_j\text{-CC}(q)\Big) = \text{true for all } j \leq i \text{ and all } q \in \alpha_i\text{-CC}(p) \Big\}.$$

Note that in [13] the condition 'and all $q \in \alpha_i$-CC(p)' was missing. The first author proposed the additional condition following a counter-example provided to him by Christian Ronse. If all predicates P_k are decreasing[3], this procedure is equivalent to checking the predicates on the α_i-CC of p only, see Eq. 4 in [13]. Indeed, once they are satisfied by the α_i-CC of p, they will be satisfied by the α_j-CC of q, because the latter are smaller or equal to the former.

Examples of decreasing predicates are 'is the difference between the largest and smallest value of the α_i-connected component below a threshold value ω?' and 'is the α_i-connected component strongly[4] connected?'. The predicate 'is the variance of the intensity values of the α_i-connected component below a given threshold level σ?' is an example of non-decreasing predicate. Additional examples of decreasing and non-decreasing predicates (similar to attribute thinnings [20]) can be found in [12,13].

From a theoretical point of view, constrained connectivity is related to the framework of the lattice approach to image segmentation proposed by Serra [21] and further investigated by Ronse [3]. More precisely, in [21] and [3], one considers

---

[3] A (logical) predicate is said to be decreasing if and only if every subset of any set satisfying this predicate also satisfies it [13].

[4] A α-connected component is strongly connected if and only if all edges of the connected components have a weight less than or equal to α (the weight of an edge between two adjacent pixels of the CC is defined as the range of the intensity values of the nodes it links).

connective segmentation, that is, segmentation methods where a connective criterion is associated to the image so that the final segmentation consists of a partition of connected components. However, connective segmentation as per [21] and [3] does not constrain the connected components in the sense of [12]. Therefore, while constrained connectivity uses a connective criterion (the α-connectivity), not all connected components resulting from this criterion are allowed but only the largest ones satisfying a series of constraints. From a theoretical point of view, the extension of the connective segmentation paradigm in order to integrate the constrained connectivity paradigm is studied mathematically in [22]. In particular, it is shown that constrained connectivity fits the framework of open-overcondensations [23].

3 Transition Pixels and Regions

The constrained connectivity paradigm partitions the image definition domain into maximal connected components satisfying a series of constraints expressed in terms of logical predicates. In practice, large connected components are often surrounded by a stream of small, usually one pixel thick, connected components. Indeed, given the general low pass filtering nature of imaging systems, ideal step edges are actually transformed (blurred) into ramp discontinuities. In the worst case, the ramp is made of steps of equal intensity so that it is pulverised into as many connected components as the number of steps (unless the creation of a large connected component encompassing the whole ramp would not violate the input connectivity constraints). Ramp pixels are sometimes called stairs [24], transition regions [25], or simply transitions [26] because they establish a path between nearby bright and dark regions. They are analogous to the notion of samples of intermediate (transitional) characteristics lying between actual clusters, see for example [27]. They are also related to the concept of mixed pixels since the intensity of a ramp pixel can be viewed as a mixture of the intensity of the regions separated by the considered ramp.

A definition of transition regions using topological and size criteria is proposed in [28]. Methods based solely on an area criterion are investigated in [10,29]. However, small regions do not necessarily correspond to transition regions. In [25], transition regions are defined as one-pixel regions having neighbouring brighter and darker regions after a preprocessing stage based on alternating sequential filters by reconstruction. In [15], transition regions are defined as connected components disappearing with an elementary erosion and not containing any regional extremum. Here, we first introduce the notion of *transition pixel*. It is then used for determining whether a given connected component correspond to a *transition region*.

A pixel of a grey level image f is a *local* extremum if and only if all its neighbours have a value either greater or lower than that of the considered pixel. That is, in morphological terms, a pixel is a local extremum if and only if the minimum between the gradients by erosion ρ^{ε} and dilation ρ^{δ} of f at position p is equal to 0:

$$p, \text{ local extremum of } f \Leftrightarrow \left[\rho^{\varepsilon}(f) \wedge \rho^{\delta}(f)\right](p) = 0. \tag{2}$$

The local extremum map LEXTR of a grey level image f is simply obtained by thresholding the pointwise minimum of its gradients by erosion and dilation for all values equal to 0:

$$\text{LEXTR}(f) = T_{t=0}[\rho^{\varepsilon}(f) \wedge \rho^{\delta}(f)]. \tag{3}$$

The LEXTR map corresponds to the indicator function returning 1 for local extrema pixels and 0 otherwise. We define transition pixels of a grey level image f as those image pixels that are *not* local extrema:

$$p, \text{ transition pixel of } f \Leftrightarrow \left[\rho^{\varepsilon}(f) \wedge \rho^{\delta}(f)\right](p) \neq 0. \tag{4}$$

The value of the morphological gradient of a transition pixel indicates the largest intensity jump that occurs when crossing this pixel. It corresponds to the intensity difference between its highest and lowest neighbours. We call *transition map* the grey tone image obtained by setting each transition pixel to the value of this intensity difference:

$$\left[\text{TMAP}(\mathbf{f})\right](p) = \begin{cases} 0, & \text{if } p \in \text{LEXTR}^1(f), \\ \left[\rho(f)\right](p), & \text{otherwise}, \end{cases} \tag{5}$$

where ρ denotes the morphological gradient operator (i.e., sum of the gradients by erosion and dilation). Interestingly, for an ideal image with regions of constant intensity levels separated by ideal step edges (and assuming that one pixel thick regions must correspond to local extrema) the transition map is equal to zero everywhere. Note that this would not be the case if regional instead of local extrema would have been considered. Finally, a transition region is defined as a constrained connected component containing only transition pixels. We present hereafter formal definitions suitable for the processing of multichannel images.

The search for local extrema in multichannel images is not straightforward because there exists no total ordering between vectors of more than one dimension. To circumvent this problem, we adopt a marginal ordering procedure whereby each channel is processed separately. Hence, when considering a multichannel image $\mathbf{f} = (f_1, \ldots, f_m)$, we define the operator LEXTR^{Σ} summing the outputs of the indicator function LEXTR applied to each channel f_j of the input image:

$$\text{LEXTR}^{\Sigma}(\mathbf{f}) = \sum_{j=1}^{j=m} \text{LEXTR}(f_j). \tag{6}$$

We then define the local extrema of order n as those pixels of the image that are local extrema in at least n channels of the input image. They are denoted by LEXTR^n:

$$\text{LEXTR}^n(\mathbf{f}) = \{p \mid \left[\text{LEXTR}^{\Sigma}(\mathbf{f})\right](p) \geq n\}. \tag{7}$$

In the following, we are interested in the local extrema of lowest order LEXTR^1. A pixel p is a transition pixel if and only if, in all channels of the input image, it has at least one lower and one higher neighbours:

$$p, \text{ transition pixel of } \mathbf{f} \Leftrightarrow p \notin \text{LEXTR}^1(\mathbf{f}) \Leftrightarrow \vee_{j=1}^{j=m} \text{LEXTR}(f_j) = 0. \tag{8}$$

That is, a pixel of a multichannel is a transition pixel if and only if it is a transition pixel in *each* individual channel.

The calculation of the maximal amplitude of the grey level difference between neighbours of each transition pixel and over all channels leads to the notion of transition map for multichannel image. Formally, it is denoted by TMAP and obtained by setting non transition pixels to 0 and transition pixels to the pointwise maximum of the morphological gradient computed for each channel:

$$[\mathrm{TMAP}(\mathbf{f})](p) = \begin{cases} 0, & \text{if } p \in \mathrm{LEXTR}^1(\mathbf{f}), \\ \bigvee_{j=1}^{j=m} [\rho(f_j)](p), & \text{otherwise.} \end{cases} \tag{9}$$

Finally, a connected component is deemed to be a transition region if it contains only transition pixels or, equivalently, if it does *not* contain any local extremum pixel appearing in any channel of the input image:

$$\begin{aligned} &(P_1, \ldots, P_n)\text{-CC}(p) \text{ is a transition region} \\ &\Leftrightarrow (P_1, \ldots, P_n)\text{-CC}(p) \cap \mathrm{LEXTR}^1 = \emptyset. \end{aligned} \tag{10}$$

This latter test can be achieved efficiently by performing the reconstruction of the labelled connected components using the complement of LEXTR^1 as seed pixels.

Once transition regions are detected, they can be removed from the partition so that the latter becomes a partial partition. The remaining non-transition regions are then expanded so as to cover again the whole image definition domain in order to obtain again a partition. This is illustrated on actual image data in the next section.

4 Experimental Results

A sample of a Landsat satellite image is displayed in Fig. 1a (only the true colour channels among the 6 available channels are considered in this experiment). The output of LEXTR^{Σ} is displayed in Fig. 1b. The grey level value of this image indicates how may times each pixel is a local extremum when considering each channel separately. It follows that the grey level values of Fig. 1b range from 0 (never a local extremum) to 3 (local extremum in all 3 channels). Figure 1c shows the output of LEXTR^1, i.e., the local extrema of order 1 of the colour image of Fig. 1a. It corresponds to the pixels of Fig. 1b having a value greater than 0.Transition pixels correspond to the white pixels of Fig. 1c. The transition map TMAP with transition pixels set to the pointwise maximum of the morphological gradient of each channel is displayed in Fig. 1d.

Figure 2a shows the constrained connected components of Fig. 1a using identical contrast values for the local $\boldsymbol{\alpha}$ and global $\boldsymbol{\omega}$ range vectors [12]: $\boldsymbol{\alpha} = \boldsymbol{\omega} = (32, 32, 32)$. The transition regions as per Eq. 10 are displayed in Fig. 2b. Once the transition regions have been detected, they are removed from the partition. The gaps of the resulting partial partition are filled thanks to a seeded region procedure [30] initiated by the non-transition regions. This procedure ensures that all transition regions are suppressed but at the cost of some arbitrary decisions in the

(a) Input colour image $\mathbf{f}$ (256×256 pixels)

(b) $\mathrm{LEXTR}^{\Sigma}(\mathbf{f})$ (grey values range from 0 to 3)

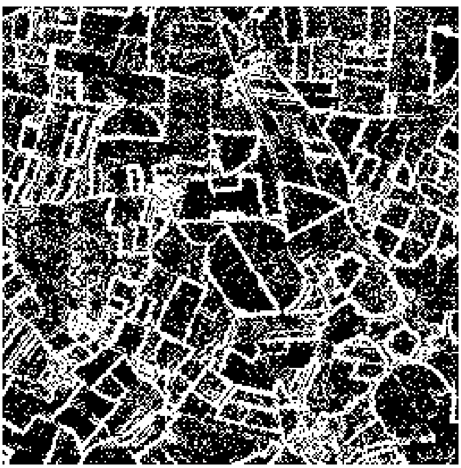

(c) $\mathrm{LEXTR}^{1}(\mathbf{f})$ (black for 1 and white for 0 values)

(d) Transition map of $\mathbf{f}$: $\mathrm{TMAP}(\mathbf{f})$

Fig. 1. Local extrema of a multichannel image (true colour channels of a Landsat image) and corresponding transition map

presence of transition regions whose smallest distance (in the spectral domain) to their neighbouring regions is obtained for more than one region. The resulting filtered partition is shown in Fig. 2c. The idea of filling the gaps of a partial partition using seeded region growing originates from [31]. In this latter case, the partial partition was obtained by removing all image iso-intensity connected components whose area is less than a given threshold value (this idea is further expanded in [29] to multichannel images and α-connected components). Figure 2d shows the simplification of Fig. 1a by setting each segment of Fig. 2c to the mean RGB value

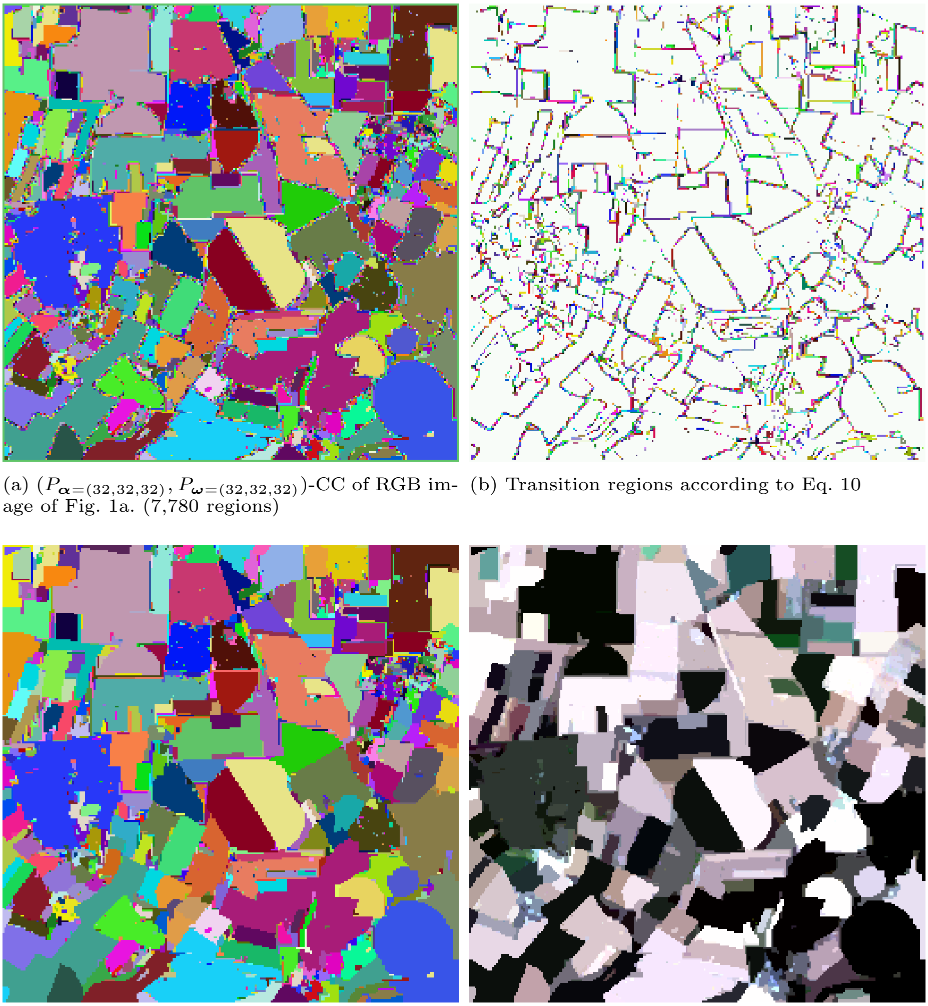

(a) $(P_{\boldsymbol{\alpha}=(32,32,32)}, P_{\boldsymbol{\omega}=(32,32,32)})$-CC of RGB image of Fig. 1a. (7,780 regions)

(b) Transition regions according to Eq. 10

(c) Filtered partition (1,669 regions)

(d) Resulting simplified RGB image

Fig. 2. From constrained connected components to transition regions and resulting edge preserving simplification (see input image in Fig. 1a)

of the input image pixels falling within this segment. The resulting image can be viewed as a sharpened image through ramp width zeroing based on region growing. Similarly, our approach can be linked to the discrete sharpening filters proposed in [32] and further developed in [33]. Indeed, the underlying ideas of the so-called Kramer-Bruckner filters consists in setting each pixel to its dilated or eroded value depending on which one is closer to its value. Consequently, for grey tone images, the sharpening transformation modifies only non-local extrema, i.e., transition pixels. More generally, a relationship can be established with the class of morphological image enhancement methods [34].

Note that transition regions also occur when generating a partition by automatically combining fine to coarse partition hierarchy using lifetime measurements [12]. Indeed, transition regions usually persist for a wide range of scale so that their lifetime is high. The concepts presented in this paper can also be used for removing these transitions regions.

5 Concluding Remarks

We have shown that the detection of constrained connected components corresponding to transition regions is of interest for segmentation and edge preserving simplification purposes. It is also useful for unsupervised classification techniques. Indeed, only those pixels not corresponding to transition regions should be considered when performing cluster analysis in a feature space to avoid overlap between clusters [35]. Similarly, the detection of transition pixels could be exploited by methods aiming at separating pure from mixed pixels. We have advocated the use of *local* extrema for marking non-transition regions. Local extrema instead of regional minima or maxima could form a basis for an interesting new type of jump connection [21,3]. Finally, we plan to analyse whether edge-preserving smoothing using a similarity measure in adaptive geodesic neighbourhoods [36,37] provides us with a valid pre-processing transformation to reduce the occurence of transition regions.

Acknowledgments

We wish to thank Christian Ronse and Jean Serra for their comments on a preliminary version of this paper as well as for email correspondence about connectivity.

References

1. Davey, B., Priestley, H.: Introduction to Lattices and Order, 2nd edn. Cambridge University Press, Cambridge (2002)
2. Zucker, S.: Region growing: childhood and adolescence. Computer Graphics and Image Processing 5, 382–399 (1976)
3. Ronse, C.: Partial partitions, partial connections and connective segmentation. Journal of Mathematical Imaging and Vision 32, 97–125 (2008)
4. Brice, C., Fennema, C.: Scene analysis using regions. Artificial Intelligence 1, 205–226 (1970)
5. Rosenfeld, A.: Fuzzy digital topology. Information and Control 40, 76–87 (1979)
6. Serra, J., Salembier, P.: Connected operators and pyramids. In: Dougherty, E., Gader, P., Serra, J. (eds.) Image Algebra and Morphological Image Processing IV. SPIE, vol. 2030, pp. 65–76 (1993)
7. Nagao, M., Matsuyama, T., Ikeda, Y.: Region extraction and shape analysis in aerial photographs. Computer Graphics and Image Processing 10, 195–223 (1979)
8. Gower, J., Ross, G.: Minimum spanning trees and single linkage cluster analysis. Applied Statistics 18, 54–64 (1969)

9. Meyer, F., Maragos, P.: Morphological scale-space representation with levelings. In: Nielsen, M., Johansen, P., Olsen, O., Weickert, J. (eds.) Scale-Space 1999. LNCS, vol. 1682, pp. 187–198. Springer, Heidelberg (1999)
10. Zanoguera, F., Meyer, F.: On the implementation of non-separable vector levelings. In: Talbot, H., Beare, R. (eds.) Proceedings of VIth International Symposium on Mathematical Morphology, Sydney, Australia, Commonwealth Scientific and Industrial Research Organisation, pp. 369–377 (2002)
11. Everitt, B., Landau, S., Leese, M.: Cluster Analysis, 4th edn. Oxford University Press, Oxford (2001)
12. Soille, P.: Constrained connectivity for hierarchical image partitioning and simplification. IEEE Transactions on Pattern Analysis and Machine Intelligence 30, 1132–1145 (2008)
13. Soille, P.: On genuine connectivity relations based on logical predicates. In: Proc. of 14th Int. Conf. on Image Analysis and Processing, Modena, Italy, pp. 487–492. IEEE Computer Society Press, Los Alamitos (2007)
14. Arora, H., Ahuja, N.: Analysis of ramp discontinuity model for multiscale image segmentation. In: Proc. of 18th International Conference on Pattern Recognition, pp. 99–103. IEEE, Los Alamitos (2006)
15. Soille, P., Grazzini, J.: Advances in constrained connectivity. In: Coeurjolly, D., Sivignon, I., Tougne, L., Dupond, F. (eds.) DGCI 2008. LNCS, vol. 4992, pp. 423–433. Springer, Heidelberg (2008)
16. Baraldi, A., Parmiggiani, F.: Single linkage region growing algorithms based on the vector degree of match. IEEE Transactions on Geoscience and Remote Sensing 34, 137–148 (1996)
17. Szczepanski, M., Smolka, B., Plataniotis, K., Venetsanopoulos, A.: On the distance function approach to color image enhancement. Discrete Applied Mathematics 139, 283–305 (2004)
18. Noyel, G., Angulo, J., Jeulin, D.: On distances, paths and connections for hyperspectral image segmentation. In: Banon, G., Barrera, J., Braga-Neto, U., Hirata, N. (eds.) Proceedings of International Symposium on Mathematical Morphology. São José dos Campos, Instituto Nacional de Pesquisas Espaciais (INPE), vol. 1, pp. 399–410 (2007)
19. Barnett, V.: The ordering of multivariate data (with discussion). Journal of the Royal Statistical Society (A) 139, 318–355 (1976)
20. Breen, E., Jones, R.: Attribute openings, thinnings, and granulometries. Computer Vision and Image Understanding 64, 377–389 (1996)
21. Serra, J.: A lattice approach to image segmentation. Journal of Mathematical Imaging and Vision 24, 83–130 (2006)
22. Ronse, C.: Block splitting operators on (partial) partitions for morphological image segmentation. Technical report, Université Louis Pasteur, Strasbourg, France (2009)
23. Ronse, C.: A lattice-theoretical morphological view on template extraction in images. Journal of Visual Communication and Image Representation 7, 273–295 (1996)
24. Crespo, J., Serra, J.: Morphological pyramids for image coding. In: Haskell, B., H.M. (eds.) Proc. Visual Communications and Image Processing. SPIE, vol. 2094, pp. 159–170 (1993)
25. Crespo, J., Schafer, R., Serra, J., Gratin, C., Meyer, F.: The flat zone approach: a general low-level region merging segmentation method. Signal Processing 62, 37–60 (1997)

26. Guimarães, S., Leite, N., Couprie, M., Araújo, A.: A directional and parametrized transition detection algorithm based on morphological residues. In: XV Brazilian Symposium on Computer Graphics and Image Processing, pp. 261–268 (2002)
27. Hodson, F., Sneath, P., Doran, J.: Some experiments in the numerical analysis of archaeological data. Biometrika 53, 311–324 (1966)
28. Strong, J., Rosenfeld, A.: A region coloring technique for scene analysis. Communication of the ACM 16, 237–246 (1973)
29. Brunner, D., Soille, P.: Iterative area filtering of multichannel images. Image and Vision Computing 25, 1352–1364 (2007)
30. Adams, R., Bischof, L.: Seeded region growing. IEEE Transactions on Pattern Analysis and Machine Intelligence 16, 641–647 (1994)
31. Soille, P.: Beyond self-duality in morphological image analysis. Image and Vision Computing 23, 249–257 (2005)
32. Kramer, H., Bruckner, J.: Iterations of a non-linear transformation for enhancement of digital images. Pattern Recognition 7, 53–58 (1975)
33. Meyer, F., Serra, J.: Contrasts and activity lattice. Signal Processing 16, 303–317 (1989)
34. Schavemaker, J., Reinders, M., Gerbrands, J., Backer, E.: Image sharpening by morphological filtering. Pattern Recognition 33, 997–1012 (2000)
35. Poggio, L., Soille, P.: Land cover classification with unsupervised clustering and hierarchical partitioning. In: 11th Int. Conf. of the International Federation of Classification Societies (IFCS): Classification as a Tool for Research, Dresden (2009), `http://www.ifcs2009.de`
36. Grazzini, J., Soille, P.: Adaptive morphological filtering using similarities based on geodesic time. In: Coeurjolly, D., Sivignon, I., Tougne, L., Dupond, F. (eds.) DGCI 2008. LNCS, vol. 4992, pp. 519–528. Springer, Heidelberg (2008)
37. Grazzini, J., Soille, P.: Edge-preserving smoothing using a similarity measure in adaptive geodesic neighbourhoods. Pattern Recognition 42, 2306–2316 (2009), `http://dx.doi.org/10.1016/j.patcog.2008.11.004`